https://doi.org/10.1364/OE.14.001957

Plasmonic field enhancement and SERS in the effective mode volume picture

Stefan A. Maier
Centre for Photonics and Photonic Materials, Department of Physics, University of Bath, Bath BA2 7AY, UK
S.Maier@bath.ac.uk

Abstract: The controlled creation of nanometric electromagnetic field confinement via surface plasmon polariton excitations in metal/insulator/metal heterostructures is described via the concept of an effective electromagnetic mode volume V_{eff}. Extensively used for the description of dielectric microcavities, its extension to plasmonics provides a convenient figure of merit and allows comparisons with dielectric counterparts. Using a one-dimensional analytical model and three-dimensional finite-difference time-domain simulations, it is shown that plasmonic cavities with nanometric dielectric gaps indeed allow for *physical* as well as *effective* mode volumes well below the diffraction limit in the gap material, despite significant energy penetration into the metal. In this picture, matter-plasmon interactions can be quantified in terms of quality factor Q and V_{eff}, enabling a resonant cavity description of surface enhanced Raman scattering.

OCIS codes: (240.6680) Surface plasmons; (230.5750) Resonators; (170.5660) Raman Spectroscopy

References and links

1. S. A. Maier and H. A. Atwater, "Plasmonics: Localization and guiding of electromagnetic energy in metal/dielectric structures," J. Appl. Phys. **98**, 011,101 (2005).
2. S. A. Maier, P. G. Kik, H. A. Atwater, S. Meltzer, E. Harel, B. E. Koel, and A. A. G. Requicha, "Local detection of electromagnetic energy transport below the diffraction limit in metal nanoparticle plasmon waveguides," Nat. Mat. **2**, 229–232 (2003).
3. W. L. Barnes, A. Dereux, and T. Ebbesen, "Surface plasmon subwavelength optics," Nature **424**, 824–830 (2002).
4. K. Kneipp, Y. Wang, H. Kneipp, L. T. Perelman, I. Itzkan, R. R. Dasari, and M. S. Feld, "Single molecule detection using surface-enhanced Raman scattering (SERS)," Phys. Rev. Lett. **78**, 1667 (1997).
5. S. M. Nie and S. R. Emery, "Probing single molecules and single nanoparticles by surface-enhanced Raman scattering," Science **275**, 1102 (1997).
6. H. Xu, J. Aizpurua, M. Kaell, and P. Apell, "Electromagnetic contributions to single-molecule sensitivity in surface-enhanced Raman scattering," Phys. Rev. E **62**, 4318–4324 (2000).
7. A. Sundaramurthy, K. B. Crozier, G. S. Kino, D. P. Fromm, P. J. Schuck, and W. E. Moerner, "Field enhancement and gap-dependent resonance in a system of two opposing tip-to-tip Au nanotriangles," Phys. Rev. B. **72**, 165409 (2005)
8. H. Kimble, "*Structure and Dynamics in Cavity Quantum Electrodynamics*," pp. 203–266 (Academic Press, Boston, 1994).
9. D. J. Norris, M. Kuwata-Gonokami, and W. E. Moerner, "Excitation of a single molecule on the surface of a spherical microcavity," Appl. Phys. Lett. **71**, 297–299 (1997).
10. R. K. Chang and A. J. Campillo, eds., *"Optical Processes in Microcavities"* (World Scientific, Singapore, 1996).
11. D. W. Vernooy, V. S. Ilchenko, H. Mabuchi, E. W. Streed, and H. J. Kimble, "High-Q measurements of fused-silica microspheres in the near infrared," Opt. Lett. **23**, 247–249 (1998).
12. D. K. Armani, T. J. Kippenberg, S. M. Spillane, and K. J. Vahala, "Ultra-high-Q toroid microcavity on a chip," Nature **421**, 925–928 (2003).

#10114 - $15.00 USD Received 3 January 2006; received 28 February 2006; accepted 28 February 2006

13. A. F. J. Levi, S. L. McCall, S. J. Pearton, and R. A. Logan, "Room Temperature Operation of Submicrometre Radius Disk Laser," Electron. Lett. **29**, 1666–1667 (1993).
14. J. D. Joannopoulos, R. D. Meade, and J. N. Winn, *"Photonic Crystals"* (Princeton University Press, Princeton, New Jersey, 1995).
15. O. Painter, R. K. Lee, A. Yariv, A. Scherer, J. D. O'Brien, P. D. Dapkus, and I. Kim, "Two-Dimensional Photonic Band-Gap Defect Mode Laser," Science **284**, 1819–1824 (1999).
16. W. Vogel and D.-G. Welsch, *"Lectures on Quantum Optics"* (Akademie Verlag GmbH, Berlin, Federal Republic of Germany, 1994).
17. E. M. Purcell, "Spontaneous emission probabilities at radio frequencies," Phys. Rev. **69**, 681 (1946).
18. A. B. Matsko, A. A. Savchenkov, R. J. Letargat, V. S. Ilchenko, and L. Maleki, "On cavity modification of stimulated Raman scattering," J. Opt. B: Quantum Semiclass. Opt. **5**, 272–278 (2003).
19. M. Kerker, D.-S. Wang, and H. Chew, "Surface enhanced Raman scattering (SERS) by molecules adsorbed at spherical particles: errata," Appl. Opt. **19**, 4159–4147 (1980).
20. B. Prade, J. Y. Vinet, and A. Mysyrowicz, "Guided optical waves in planar heterostructures with negative dielectric constant," Phys. Rev. B **44**, 13,556–13,572 (1991).
21. P. B. Johnson and R. W. Christy, "Optical constants of the noble metals," Phys. Rev. B **6**, 4370–4379 (1972).
22. R. Loudon, "The propagation of electromagnetic energy through an absorbing dielectric," J. Phys. A **3**, 233–245 (1970).
23. R. Ruppin, "Electromagnetic energy density in a dispersive and absorptive material," Phys. Lett. A **299**, 309–312 (2002).
24. J. Takahara, S. Yamagishi, H. Taki, A. Morimoto, and T. Kobayashi, "Guiding of a one-dimensional optical beam with nanometer diameter," Opt. Lett. **22**, 475 (1997).
25. L. C. Andreani, G. Panzarini, and J.-M. Gérard, "Strong-coupling regime for quantum boxes in pillar microcavities: Theory," Phys. Rev. B **60**, 13,276 (1999).
26. M. A. Ordal, L. L. Long, R. J. Bell, R. R. Bell, R. W. Alexander, and C. A. Ward, "Optical properties of the metals Al, Co, Cu, Au, Fe, Pb, Ni, Pd, Pt, Ag, Ti, and W in the infrared and far infrared," Appl. Opt. **22**, 1099–1119 (1983).
27. I. A. Larkin, M. I. Stockman, M. Achermann, and V. I. Klimov, "Dipolar emitters at nanoscale proximity of metal surfaces: Giant enhancement of relaxation in microscopic theory," Phys. Rev. B **69**, 121403(R) (2004).
28. H. A. Haus, *"Waves and Fields in Optoelectronics"*, 1st ed. (Prentice-Hall, Englewood Cliffs, New Jersey 07632, 1984).
29. S. M. Spillane, T. J. Kippenberg, and K. J. Vahala, "Ultralow-threshold Raman laser using spherical dielectric microcavity," Nature **415**, 621–623 (2002).
30. T. Klar, M. Perner, S. Grosse, G. von Plessen, W. Spirkl, and J. Feldmann, "Surface-plasmon resonances in single metallic nanoparticles," Phys. Rev. Lett. **80**, 4249–4252 (1998).
31. V. A. Shubin, W. Kim, V. P. Safonov, A. K. Sarychev, R. L. Armstrong, and V. M. Shalaev, "Surface-plasmon-enhanced radiation effects in confined photonic systems," J. Lightwave Technol. **17**, 2183–2190 (1999).
32. E. Hinds, *"Pertubative cavity quantum electrodynamics"*, pp. 1–56 (Academic Press, Boston, 1994).
33. W. L. Barnes, "Electromagnetic Crystals for Surface Plasmon Polaritons and the Extraction of Light from Emissive Devices," J. Lightwave Technol. **17**, 2170–2182 (1999).
34. J. Vučković, M. Lončar, and A. Scherer, "Surface plasmon enhanced light-emitting diode," IEEE J. Quantum Electron. **36**, 1131–1144 (2000).

1. Introduction

In recent years, the ever-increasing research efforts in the field of *plasmonics* - the study of electromagnetic field confinement and enhancement via surface plasmon polaritons (SPPs) - have led to a number of important advances towards the goal of a nanophotonic infrastructure for confining and guiding electromagnetic radiation [1]. Recent examples include the creation of metal nanoparticle plasmon waveguide [2] and other sub-wavelength photonic devices [3], the fabrication of which is enabled by nanofabrication tools such as electron beam lithography. However, one of the most prominent application of SPPs and localized plasmons, single molecule surface enhanced Raman scattering (SERS)[4, 5], has up to now not been described in a context of field enhancement in *designed* metal nanoscale cavities. The single molecule sensitivity relies on light localization in hot-spots on a roughened silver (Ag) surface where random, nanometer-sized junctions between surface protrusions are believed to form cavity-like structures for field enhancement [6]. As a step towards a controlled sensing platform for SERS [7], here the enhancement process is presented from a waveguide-to-cavity-coupling point of view,

#10114 - $15.00 USD Received 3 January 2006; received 28 February 2006; accepted 28 February 2006

which requires a careful look at the energetics of plasmonic energy localization in metallic nanocavities.

Optical cavities in general provide an intriguing way to alter the interaction of light with matter and have been employed in a wide range of fields from cavity quantum electrodynamics (cQED) [8] to single-molecule sensing [9]. As is well known from work on dielectric resonant cavities, a given cavity can be characterized in terms of its quality factor Q, being proportional to the cavity photon lifetime, and its effective mode volume V_{eff}, quantifying the electric field strength per photon. Q and $1/V_{\text{eff}}$ can be thought of as the spectral and spatial energy density of the resonant mode, respectively. Prominent geometries include dielectric spheres [10, 11], microtoroids [12], microdisks [13], and dielectric photonic crystals [14]. The former can sustain very high quality factors $Q > 10^8$ enabling $Q/\bar{V}_{\text{eff}} \sim 10^5$ [12], where $\bar{V}_{\text{eff}}$ is the effective mode volume normalized to $(\lambda_0/n)^3$, the cubic wavelength in the material. Photonic crystal microcavities on the other hand allow V_{eff} to approach the theoretical diffraction limit, corresponding to a cubic half wavelength in the material [15].

In a quasi-normal mode picture [16], one can quantify the coupling between matter and the electromagnetic field of a resonant cavity using Q and V_{eff}. The beauty of this approach lies in the ability to determine simple scaling laws for various processes such as spontaneous emission [17], strong matter-photon coupling [8] and non-linear optical thresholds [18] in terms of these two parameters. In order to compare and contrast plasmonic resonant structures with their dielectric counterparts, here this formalism will be carried over to the description of interactions between matter and surface plasmon-polaritons. Of critical importance to the mode expansion analysis is the careful determination of V_{eff} for metallic systems, where the generation of localized light volumes smaller than the diffraction limit in the dielectric space surrounding a metallic nanostructure does not in itself imply that V_{eff} is smaller than the diffraction limit. The applicability of the effective mode volume concept for metallic nanostystems requires careful account of the dispersive character of the plasmon-polariton excitations and the electromagnetic energy *stored inside the metal*, both of which become significant for deep sub-wavelength confinement. After a discussion of a nanoplasmonic Fabry-Perot type resonator using both a onedimensional analytical model and threedimensional finite difference time domain (FDTD) simulations, the advantages of characterizing plasmonic energy confinement in terms of Q and V_{eff} are demonstrated via a simple model for surface enhanced Raman scattering (SERS), which has typically been analyzed using scattering-type calculations [19]. The new approach is in quantitative agreement with full-field calculations for crevices between nearly touching metallic nanoparticles [6], and offers guidance in the design of individually addressable metallic and dielectric cavities for sensing purposes.

2. Onedimensional model of gap plasmons

Possibly one of the simplest geometries for a plasmonic nanoresonator allowing reproducible fabrication is that of a thin dielectric layer sandwiched between two metallic claddings (Fig. 1, left inset). In the vertical z-direction perpendicular to the plane of the dielectric core, the mode is confined via a coupled surface plasmon-polariton sustained by the metallic boundaries. Laterally, the physical extent of the cavity together with the increased wave vector of the surface plasmon mode propagating in the x-direction will lead to confinement, while in propagation direction the mode can be confined using reflective walls or indeed a simple air boundary, leading to Fabry-Perot type oscillations. Before embarking on a numerical analysis of such a cavity, it is instructive to analytically consider the energy confinement properties of a canonical planar metal-air-metal heterostructure composed out of an air ($\varepsilon_1 = 1$) core of width $2a$ surrounded by two metallic half-spaces (Fig. 1, right inset). As is well known, such a heterostructure can support two surface modes propagating in the x-direction parallel to the interfaces that are set

#10114 - $15.00 USD Received 3 January 2006; received 28 February 2006; accepted 28 February 2006

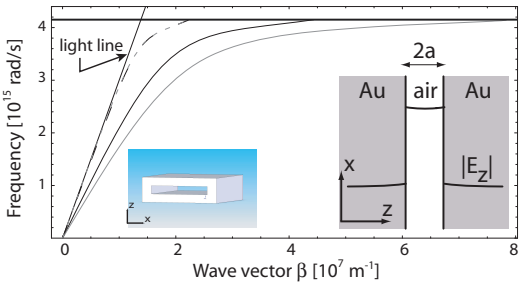

Fig. 1. Dispersion relation of the odd plasmon-polariton gap mode sustained by two infinite Au half spaces separated by an air gap $2a$ (inset) for: $2a = 1\mu$m (broken black line), 100 nm (black line), and 50 nm (gray line). Also shown is the dispersion for a single interface (broken gray line). For large wave vectors, the frequency of the mode approaches the Au/air surface plasmon frequency (horizontal line).

up by coupling of the surface plasmon-polariton modes of the individual air/metal boundaries [20]. Here the focus will be on the mode of odd *vector* parity, which does not have a cut-off gap size and shows a symmetric scalar field distribution of the dominant electric field component, E_z, with respect to the symmetry plane, as depicted in the right inset of Fig. 1 (this is the lowest order *capacitor*-type mode). The dielectric response of the metallic half-spaces is modeled using a Drude fit to the dielectric function $\varepsilon(\omega)$ for gold (Au) at visible and near-infrared frequencies [21]. The dispersion of this mode is given by the implicit relation between the propagation constant $\beta = k_x$ and the dielectric response of the metal cladding and air gap via

$$\tanh(wa) = -\frac{\varepsilon_1}{\varepsilon(\omega)}\frac{u}{w}, \tag{1}$$

where $u = \sqrt{\beta^2 - k^2\varepsilon(\omega)}$ and $w = \sqrt{\beta^2 - k^2\varepsilon_1}$. The electromagnetic energy stored in the electric field inside the metal can be calculated using an electromagnetic energy density appropriate for a highly dispersive, lossy material [22, 23] as

$$u_{\mathrm{E}} = \frac{\varepsilon_0}{2}\left(\varepsilon_1 + \frac{2\omega\varepsilon_2}{\gamma}\right)|\mathbf{E}|^2. \tag{2}$$

Here, $\varepsilon(\omega) = \varepsilon_1(\omega) + i\varepsilon_2(\omega)$ is the complex dielectric function of a Drude model with damping contant γ.

Figure 1 shows the dispersion relation of the capacitor-like mode for varying gap sizes. The dispersion for a single interface is also shown (broken gray line), which is seen to coincide with the dispersion for large gap sizes. An important point to note here is that large propagation constants β can be achieved even for excitation far below the bulk metal plasma frequency provided that the gap width is chosen sufficiently small. The ability to access such large wavevectors by adjusting the geometry indicates, as has been pointed out in previous work on sub-wavelength guiding structures [24], that localization effects that for a single interface can only be sustained at excitations near the material plasma resonance, can for this gap structure also be attained for excitation out in the the mid- and far-infrared. As will be seen below, this highly dispersive region of the bandstructure has a significant impact upon the effective mode size.

Figure 2(a) shows the evolution of both the real and imaginary parts of the β with varying gap size for excitation at a free space wavelength of $\lambda_0 = 850$nm. Both parts are seen to increase with decreasing gap size, suggesting that the capacitor mode is becoming more electron-plasma

#10114 - $15.00 USD Received 3 January 2006; received 28 February 2006; accepted 28 February 2006

in character, and that the electromagnetic energy is residing increasingly in the metal half-spaces. A plot of the fractional amount of energy inside the metal regions is shown in Fig. 2(b) for excitation at wavelengths $\lambda_0 = 600$ nm, 850 nm, 1.5 μm, 10 μm, and 100 μm ($= 3$THz), reaching e.g. 40% for a gap of 20 nm at $\lambda_0 = 850$ nm. For this and all following figures, the gap size is normalized to the respective free space wavelength, and the results for each wavelength are plotted over the range of convergence of the analytical model. It can be seen then, that along with the increased localization of the field to the metal/air interface, either via small gap sizes or excitation closer to the surface plasmon frequency, comes a shift of the energy into the metal regions.

3. Electromagnetic energy density and the effective mode volume in plasmonics

In order to get a better handle on the consequences of increasing fractions of the total energy of the mode entering the metallic cladding upon decreasing size of the dielectric gap, and to determine the overall effect on the scaling of the electric field strength per photon (more accurately, per plasmon-polariton excitation) in the air gap as a function of the gap size, one can define in analogy to the effective mode *volume* V_{eff} of cQED [25], an effective mode *length* L_{eff} for this one dimensional "resonator",

$$L_{\text{eff}}(z_0)u_{\text{E}}(z_0) = \int u_{\text{E}}(z)dz. \tag{3}$$

Here $u_{\text{E}}(z_0)$ represents the electric field energy density at position z_0, corresponding to the position of interest within the cavity. For the structure of Fig. 1, z_0 resides in the air gap where an object may be placed to interact with the field. Fig. 2(c) shows the variation of L_{eff} (normalized to the free space wavelength λ_0) with normalized gap size for the capacitor mode.

As can be seen, the mode lengths drop well below $\lambda_0/2$, demonstrating that plasmonic metal structures do indeed sustain *effective* as well as *physical* mode lengths below the diffraction limit of light. The trend in L_{eff} with gap size tends to scale with the physical extent of the air gap. For large normalized gap sizes and low frequencies, this is due to the delocalized nature of the surface plasmon, leading to smaller mode lengths for excitation closer to the surface plasmon resonance frequency for the same normalized gap size. As the gap size is reduced to a point where the bandstructure of the capacitor mode turns over (see Fig. 1) and energy begins to enter the metallic half spaces, the continued reduction in mode length is due to an increase in field localization to the metal-air surface. In this regime, excitations with lower frequencies show smaller mode lengths for the same normalized gap size than excitations closer to the plasmon resonance, due to the fact that more energy resides inside the metal for the latter. Fig. 2(d) further elucidates this effect by showing the contributions of the electric field energy in air (continuous line) and in the metal (broken line) to the total effective mode length for two excitation wavelengths.

Note that while the Drude fit to the visible and near-IR dielectric response of Au may not accurately represent the response at THz frequencies in actual numbers, the general trend that the imaginary part of the dielectric constant is significantly larger than the absolute value of the real part in this regime is well modeled, and an analysis using a Drude model more adapted to the far infrared response of Au [26] yielded mode lengths of similar magnitude. Regarding application of these results to gaps $< 1-2$ nm, in such cases it has been noted [27] that the effects of local fields due to unscreened surface electrons become important, leading to a further decrease in L_{eff} which cannot be captured using the dielectric function approach.

The present gap structure can be converted into a three-dimensional resonator, as depicted in the right inset of Fig. 1, by inserting reflecting walls parallel to the $\hat{x}$-direction, thus confining the propagation of the odd mode to a cavity length L_x. Assuming in a first approxi-

#10114 - $15.00 USD Received 3 January 2006; received 28 February 2006; accepted 28 February 2006

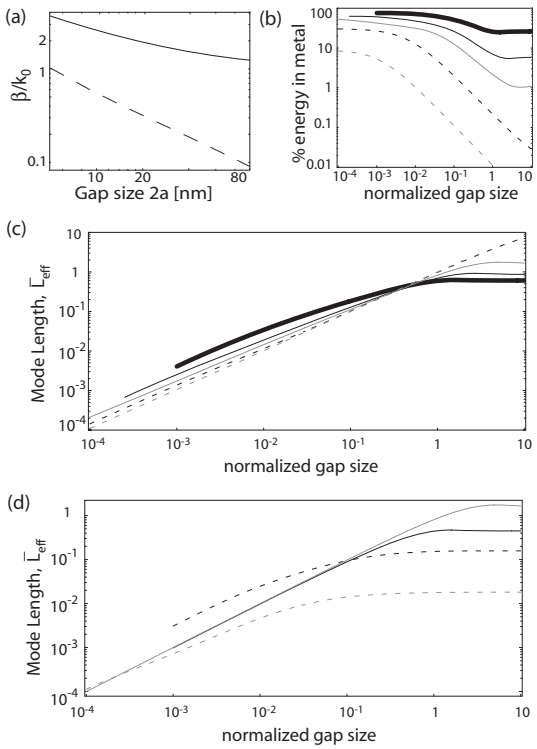

Fig. 2. (a) Normalized propagation constant β versus gap size at $\lambda_0 = 850$nm. Both the real (solid curve) and the imaginary (broken curve, 10x) part of β are seen to increase for decreasing gap. (b) Fractional electric field energy residing inside the metallic half spaces as a function of normalized gap size for excitation at $\lambda_0 = 600$ nm (thick line), 850nm (black line), 1.5 μm (gray line), 10 μm (broken black line), and 100 μm (broken gray line). (c) Effective mode length L_{eff} normalized to free space wavelength λ_0. (d) Effective mode length in the air gap (continuous line) and in the surrounding metal (broken line) for $\lambda_0 = 600$ nm (black line) and 1.5 μm (gray line).

mation perfectly reflecting cavity walls, the fundamental cavity mode will be excited when $L_x = \pi/\beta(\lambda_0, a)$. If one conservatively assumes a diffraction-limited lateral resonator width $L_y = \lambda_0/2$, the cavity mode volume can thus be approximated as $V_{\text{eff}} \sim L_{\text{eff}}(\pi\lambda_0/2\beta)$.

Another important parameter for the characterization of a resonant cavity is its quality factor Q, defined as the ratio of stored energy to loss per cycle. Assuming no radiative losses from the resonator edges and perfectly reflecting cavity walls, Q is limited by dissipative losses inside the metal alone: $Q = \omega_0/(2v_{\text{gr}}\text{Imag}(\beta))$, where v_{gr} is the group velocity of the guided mode between the metal plates. As a cavity figure of merit, Fig. 3 shows the analytically calculated $Q/\bar{V}_{\text{eff}}$. As can be seen, $Q/\bar{V}_{\text{eff}}$ greatly increases for decreasing gap size, due to the fact that $\bar{V}_{\text{eff}}$ decreases much more strongly than Q. For a resonator with $2a = 50$nm designed for excitation at $\lambda_0 = 850$nm, the analytic model predicts a $Q \sim 51$ and a normalized mode volume $\bar{V}_{\text{eff}} \sim 0.015$, leading to $Q/\bar{V}_{\text{eff}} \sim 3400$. Excitation at mid- and far-infrared frequencies can yield $Q/\bar{V}_{\text{eff}} \gg 10^4$ for similar gap sizes.

The validity of the analytical approximations employed above was confirmed via 3D FDTD simulations of this resonator structure. The inset of Fig. 3 shows the calculated mode profiles for a resonator of the same geometrical parameters employed in the analytic example. The metallic

#10114 - $15.00 USD Received 3 January 2006; received 28 February 2006; accepted 28 February 2006

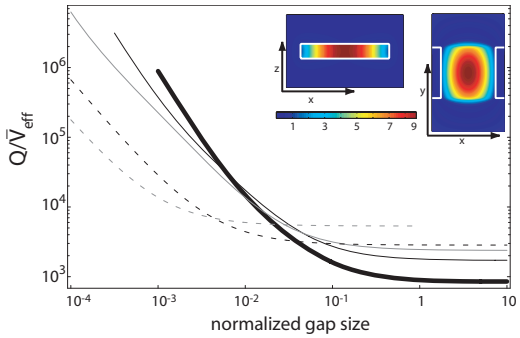

Fig. 3. Ratio of Q to V_{eff} for a 3D gap resonator of varying normalized gap size for the five excitation wavelengths of Fig. 2. The inset shows a FDTD calculated electric field intensity of a resonator with $2a = 50$nm and $\lambda_0 = 980$nm.

Au half-spaces were modeled with the same Drude function used in the analytic calculations; however, the reflecting mirror walls were in this case taken to be non-perfect, consisting also of Au. As a result, the resonance wavelength shifts from $\lambda_0 = 850$nm to 980nm due to the electric field penetration into the end mirrors. The calculated absorptive $Q_{\text{abs}} \sim 40$ is of similar magnitude as the analytic result, and a radiative $Q_{\text{rad}} \sim 100$ is found due to lateral leakage of radiation. The FDTD-calculated mode volume $\bar{V}_{\text{eff}} \sim 0.009$ is also in good agreement with the analytic model estimate when scaled by the cube of the increase in resonance wavelength. While these discussions have focused on a planar metal/insulator/metal heterostructure, the general conclusions regarding $Q/\bar{V}_{\text{eff}}$ are also expected to hold for more complicated geometries involving two metallic surfaces separated by a nanoscale gap, such as e.g. nanoshells.

4. Application to surface-enhanced Raman scattering

One is now in a position to sketch as an example of the usefulness of the effective mode volume picture to describe plasmonic energy localization its application to SERS. A spontaneous Raman scattering process involves an incoming excitation beam of intensity $|\mathbf{E}_i(\omega_0)|^2/2\eta$ (η the impedance of free space) and frequency ω_0, leading to the emission of Stokes photons at frequency ω through a Raman active molecule. Due to the small Stokes emission shift, one usually assumes equal enhancement of the exciting field and the outgoing Stokes field, and a commonly used expression[19] for the enhancement of the Raman cross section is $R = |\mathbf{E}_{\text{loc}}|^4/|\mathbf{E}_i|^4$, where $|\mathbf{E}_{\text{loc}}|$ is the local field amplitude at the Raman active site. For this treatment, $Q(\omega_0)$=$Q(\omega)$=Q and $V_{\text{eff}}(\omega_0)$=$V_{\text{eff}}(\omega)$=V_{eff}, and it is thus assumed that both the incoming and the emitted photon are resonant with the cavity.

With $|s_+|^2 = |\mathbf{E}_i|^2 A_i/2\eta$ being the power carried by the incident beam of cross section A_i, the evolution of the *on-resonance* mode amplitude u inside the cavity can be calculated from [28], $\dot{u}(t) = -\frac{\gamma}{2}u(t) + \kappa s_+$, where u^2 represents the total time-averaged energy in the cavity, $\gamma = \gamma_{\text{rad}} + \gamma_{\text{abs}}$ is the energy decay rate due to radiation (γ_{rad}) and absorption (γ_{abs}), and κ is the coupling coefficient to external input which depends on the size and shape of the excitation beam. κ can be expressed as $\kappa = \sqrt{\gamma_i}$, where γ_i is the contribution of the excitation channel to the total radiative decay rate [28]. For a symmetric two-sided cavity, in a first approximation one can estimate $\gamma_i = (\gamma_{\text{rad}}/2)(A_c/A_i)$, with A_c corresponding to an effective radiation cross-section of the resonant cavity mode (its radiation field imaged back into the near-field of the cavity). Note that A_i has been assumed to be larger than A_c in the above relation, and that A_c can be no smaller than the diffraction limited area A_d, yielding $A_d \leq A_c \leq A_i$. In steady state,

#10114 - $15.00 USD Received 3 January 2006; received 28 February 2006; accepted 28 February 2006

the mode amplitude can then be expressed as

$$u = \frac{\sqrt{2\gamma_{\rm rad}A_c/A_i}|s_+|}{\gamma_{\rm rad}+\gamma_{\rm abs}} = \frac{\sqrt{\gamma_{\rm rad}A_c}|\mathbf{E}_i|}{\sqrt{\eta}(\gamma_{\rm rad}+\gamma_{\rm abs})}, \tag{4}$$

which for fixed incoming power is maximum upon spatial mode matching ($A_c = A_i$). For a dielectric cavity ($\gamma_{\rm rad} \gg \gamma_{\rm abs}$), one thus gets $u \propto 1/\sqrt{\gamma_{\rm rad}} \propto \sqrt{Q}$, while for a metallic cavity ($\gamma_{\rm abs} \gg \gamma_{\rm rad}$) $u \propto 1/\gamma_{\rm abs} \propto Q$, explaining the different scaling laws for field enhancement in dielectric [29] and metallic [30] resonators encountered in the literature. From the definition of effective mode volume one can write the resonant mode amplitude as $u = \sqrt{\varepsilon_0}|\mathbf{E}_{\rm loc}|\sqrt{V_{\rm eff}}$, which gives for the enhancement of the incoming radiation in a metallic cavity

$$\sqrt{R} = \frac{|\mathbf{E}_{\rm loc}|^2}{|\mathbf{E}_i|^2} = \frac{\gamma_{\rm rad}A_c}{4\pi^2c^2\eta\varepsilon_0\lambda_0}\frac{Q^2}{V_{\rm eff}}. \tag{5}$$

A similar scaling law has previously been obtained for plasmonic energy localization in fractal-like metal nanoparticle aggregates on metal surfaces [31]. Setting $A_c = A_d$ yields for our example Au resonator, with $2a = 50$ nm and $\lambda_0 = 980$ nm, an estimated SERS cross section enhancement of $R \sim 1600$.

A similar estimate of R for a crevice between two Ag nanoparticles separated by a nanoscale gap, a configuration which is believed to sustain SERS hot-spots with $R \sim 10^{11}$ upon resonance, can also be obtained using the effective mode volume picture. The crevice can be approximately modeled using the capacitor-like cavity described above, but with a reduced lateral width $L_y \sim L_x = \pi/\beta$. For a 1 nm gap, with $\lambda_0 = 400$nm, $A_c = A_d$, and $(Q, \gamma_{\rm rad})$ estimated from FDTD, eq. (5) yields $R \sim 2.7 \times 10^{10}$, in good agreement with full-field three-dimensional simulations of the enhancement for this coupled particle geometry [6]. The total observable enhancement of the Stokes emission can be estimated as the product of the field enhancement of the incoming radiation and the enhanced radiative decay rate at the Stokes frequency. As is well known, a dipole oscillator placed inside a metallic cavity shows an increase in its *total* decay rate $\gamma/\gamma_0 = (3/4\pi^2)(Q/V_{\rm eff})$[32]. For collection of light emission outside the cavity, the overall cavity enhancement is weighted with an extraction efficiency, $Q/Q_{\rm rad}$[33, 34]. Thus, the emission enhancement at the *peak* emission frequency of the Stokes line is $(3/4\pi^2)(Q^2/V_{\rm eff})(Q/Q_{\rm rad})$. Incorporating the relation for incoming field enhancement from eq. (5), the overall enhancement is estimated to be 1.5×10^{12} for the crevice example, similar to observed values[5, 4].

5. Conclusion

The description of controlled spatial electromagnetic energy localization via an effective mode volume - traditionally applied to (non-dispersive) dielectric resonators - has been extended to metallic cavities sustaining surface plasmon-polaritons and applied to the description of SERS. Using a simple model of a nanoscale plasmonic resonator with a realistic material dielectric response function, it has been demonstrated that plasmonic cavities can indeed confine electromagnetic energy into both physical and effective mode volumes far below the diffraction limit. Large $Q/V_{\rm eff}$ values can be achieved for nanometric gap sizes in metal/dielectric/metal heterostructures. Furthermore, the field enhancement due to interactions between closely spaced metallic interfaces of more complicated geometries such as nanoparticles can be estimated in these terms. This unified description of enhancement effects in both dielectric and metallic resonators will help in establishing new design principles for nanophotonic devices.

Acknowledgments

Thanks are expressed to Oskar Painter for stimulating discussions. This work was in part funded by the UK Engineering and Physical Sciences Research Council (EPSRC).

#10114 - $15.00 USD Received 3 January 2006; received 28 February 2006; accepted 28 February 2006